Proc. Indian Acad. Sci. (*Chem. Sci.*), Vol. 115, Nos 5 & 6, October–December 2003, pp 663–677

Structure of solid monolayers and multilayers of *n*-hexane on graphite¶

M KRISHNAN[1], S BALASUBRAMANIAN[1]* and S CLARKE[2]
[1]Chemistry and Physics of Materials Unit, Jawaharlal Nehru Centre for Advanced Scientific Research, Jakkur PO, Bangalore 560 064, India
[2]Department of Chemistry and BP Institute, Madingley Rise, Madingley Road, University of Cambridge, Cambridge CB3 0HE, UK
e-mail: bala@jncasr.ac.in

Abstract. We present all-atom molecular dynamics simulations of *n*-hexane on the basal plane of graphite at monolayer and multilayer coverages. In keeping with experimental data, we find the presence of ordered adsorbed layers both at single monolayer coverage and when the adsorbed layer coexists with excess liquid adsorbate. Using a simulation method that does not impose any particular periodicity on the adsorbed layer, we quantitatively compare our results to the results of neutron diffraction experiments and find a structural transition from a uniaxially incommensurate lattice to a fully commensurate structure on increasing the coverage from a monolayer to a multilayer. The zig-zag backbone planes of all the alkane molecules lie parallel to the graphite surface at the multilayer coverage, while a few molecules are observed to attain the perpendicular orientation at monolayer coverage.

Keywords. *n*-Hexane; graphite; adsorption; monolayer commensurate; simulation.

1. Introduction

The *n*-alkanes exhibit an interesting variety of phase behaviour in the bulk, with particular structural differences between alkanes that have an even number of carbon atoms and those that have an odd number.[1] The origin of such odd–even effects in three-dimensional molecular materials has been attributed to differences in the strengths of the methyl-methyl interactions to the ones between methylene groups.[2] This interplay between the interaction strengths of different groups in *n*-alkanes is accentuated in the presence of a surface. Graphite is well suited to study the evolution of the structure of *n*-alkanes, as alkanes can adsorb in a commensurate manner, due to the fact that one of the lattice constants of graphite (2·46 Å) is quite close to the 1–3 distance (the distance between methylene groups separated by one CH_2 group is about 2·54 Å) in a linear alkane.[3] This enables nearly all the methylene groups of *n*-alkanes to adsorb at preferred sites on the graphite lattice. The long chain *n*-alkanes are industrially important as lubricants to prevent wear of metal surfaces at close contact, thus making the study of their behaviour under confinement a matter of great importance.[4–6] The phase behaviour of solid monolayers of single and multi-component short chain *n*-alkanes have been extensively studied recently.[7]

¶Dedicated to Professor C N R Rao on his 70th birthday
*For correspondence

n-Hexane crystallises in a herringbone pattern on graphite. Hansen and Taub[8] and Herwig *et al*[9] have studied the mechanism of melting in *n*-butane and *n*-hexane monolayers on graphite using both neutron diffraction experiments and molecular dynamics (MD) simulations. They concluded that the melting of such short alkanes proceeds by the creation of vacancies and thus theories of melting that are strictly two dimensional are inapplicable to such systems. In an extensive study of the structure of *n*-hexane monolayers on graphite, Hansen *et al*[10] have shown that the low temperature phase is herringbone ordered, and that on increasing temperature it transforms into a rectangular centred structure that coexists with the liquid phase. Peters and Tildesley[11] have studied the melting of hexane monolayer using MD simulations. They found that the anisotropic united atom model produces the same herringbone configuration at low temperatures as an isotropic model. They also found that the monolayer described by either model melts at approximately 175 K, with subtle structural differences between the two cases. Peters[12] has also studied the melting and other phase behaviour of a *n*-hexane bilayer on graphite, and have observed that the melting point of a bilayer is increased by about 20 K with respect to that of the monolayer.

Low energy electron diffraction and neutron scattering[13,14] experiments of *n*-hexane adsorbed on graphite have shown a rather interesting dependence of the structure of the first adsorbed layer upon coverage. Quite close to monolayer coverages, the *b*-parameter of the lattice decreases significantly, by about 0·35 Å, i.e., by 7%. The compression is associated also with a transition from a structure that is uniaxially incommensurate with the underlying graphite lattice to one that is fully commensurate. Such a transition in the structure of the first adsorbed layer has also been observed recently in neutron scattering studies of other even and odd alkanes adsorbed on graphite at submonolayer coverages and at multilayer coverages.[14]

To understand this phenomenon and to provide microscopic details, we have performed atomistic molecular dynamics (MD) simulations of *n*-hexane on graphite at two coverages. The simulations described here differ significantly from earlier works[8–12] in their purpose. Our intention is to reproduce the experimental observation of the lateral compression of the *n*-hexane lattice upon increase in coverage, in as independent a manner as possible. In pursuit of this aim, we have performed MD simulations of a large cluster of *n*-hexane molecules on graphite, using the all-atom interaction model. In anticipation of the results, we observe this important compression in our simulations. The next section describes the details of the simulation, followed by results and discussion.

A preliminary account of this work has appeared elsewhere.[15] Complete details of the calculations and procedures adopted in the analyses, including the calculation of structure factor from atomic coordinates are provided here. The current work also includes results of simulations of monolayers of *n*-hexane on graphite, that employed periodic boundary conditions (PBC). A comparison of the results obtained from simulations with and without the use of PBCs enable us to independently verify the assumptions underlying the MD simulations, and its relationship to experiments. The current work, in addition, contains results of simulations that were started with 'reversed' initial configurations for the monolayer and for the multilayer, so that issues related to adequate sampling of configurational space can be resolved.

2. Simulation details

We have studied *n*-hexane on graphite at two coverages; One, a full monolayer, and the other, a system containing three layers of *n*-hexane, hereafter called the multilayer. These simulations have been performed at low temperatures and also at temperatures where the bulk alkane would be liquid. Simulations of adsorbed species on surfaces are usually performed with periodic boundary conditions. However, such simulations force a periodicity on the system and it is not possible to obtain an independent validation of experimentally determined unit cell parameters.

In these simulations, one cannot use a Parrinello–Rahman type of a procedure (also called the constant stress ensemble)[16] for a two-dimensional system in the presence of an external corrugated potential representing the surface. This is because, on a surface, the simulation box length has to be an integral multiple of the periodicity of the external potential that represents the surface, which is inconsistent with the continuous change in box size that the constant stress ensemble demands. Thus, to obtain structural data that is independent of the initial selection of the dimensions of the simulation box, the simulations were performed *without* the use of periodic boundary conditions in any of the three spatial directions, i.e., simulations were essentially carried out for a cluster of *n*-hexane molecules adsorbed on graphite. The molecules on the surface of such a cluster can, in principle, evaporate into the gas phase, depending on the vapour pressure of the system. Given the strongly attractive nature of the interaction of the molecules with the graphite substrate, the hexane molecules are unlikely to desorb from the surface. However, in the absence of periodic boundary conditions in the lateral directions, molecules at the periphery of the cluster can leave the cluster, but still be on the surface. We do not include such molecules in our analyses of the structure factor and other quantities. Cheng and Klein[17] have employed such a methodology of not using periodic boundary conditions in all three directions to study the melting of ethylene on graphite. Earlier simulations[8–10] to study the phase behaviour of *n*-hexane and other small alkanes on graphite have consistently employed periodic boundary conditions, with the cell parameters either obtained from experiments, or from static calculations. We have consciously chosen not to impose a periodicity on the simulated samples, as our primary purpose has been to reproduce the lattice compression as *independently* as possible from experiments.

For computational efficiency, one has to study a cluster that is large enough such that the ratio of molecules that are on the surface to those in bulk is reasonably small. The monolayer system studied here, consists of 350 molecules with linear dimensions in the lateral directions of 126 and 90 Å. The three-layer system consisted of 360 hexane molecules, with lateral dimensions of 71 and 91 Å. The system sizes studied here are comparable to the domain sizes of adsorbed alkanes on graphite, which is around 100 to 200 Å.[10] Recent calorimetry results have indicated that only a few additional layers are required to obtain a reasonable approximation to the bulk properties of alkanes.[18] We use three layers instead of just a bilayer to make sure that we have a complete second layer during the course of the simulation. The possibility of molecules desorbing during the high temperature annealing exists, and this could lead to voids in the second layer of a bilayer simulation. This could expose the molecules of the first layer, and might influence the structural transition that we anticipate. We have used three layers to avoid this possibility, however rare desorption might be.

For comparison with the simulations without the use of periodic boundary conditions, we have performed MD calculations of *n*-hexane on graphite at monolayer and two-layer coverages *with* the use of periodic boundary conditions. As explained succinctly in refs (10, 19), in this case the simulation box has to be an integer multiple of both the graphite unit cell as well as that of the adsorbate unit cell. We have used lattice parameters obtained from experiments for these quantities. The monolayer simulations with periodic boundary conditions were performed in a box of linear dimensions $105{\cdot}78 \times 102{\cdot}26$ Å, which corresponds to 120 unit cells of the *n*-hexane lattice. The number of atoms in the simulation was 4800. The multilayer simulations were performed for two layers of *n*-hexane adsorbed on graphite, each containing 150 molecules in a box of linear dimensions $73{\cdot}80 \times 85{\cdot}22$ Å, with a system size of 6000 atoms. The systems were equilibrated for 800 ps at 70 K, after which the structure factor of *n*-hexane was averaged over 250 ps.

The MD simulations were performed under constant temperature conditions using the Nosé–Hoover chains method,[20] with a thermostat time constant of 1 ps. An all-atom potential[21] was used for the hexane molecules and the interaction of the alkane atoms with graphite was represented by the anisotropic Steele potential.[22,23] The σ and ϵ of the surface interactions in the Steele potential were chosen to be 3·3 Å and 47·72 K for carbon and 2·98 Å and 17·0 K for hydrogen respectively. The all-atom potential has bond stretching, bending, and torsional terms apart from a non-bonded term of the 6-exponential form. The simulations had no distance constraints between atoms in a molecule, thus necessitating a timestep of integration of 0·5 fs, which was determined by the fastest degree of freedom, i.e., the C–H vibration. The potentials of interaction between sites on alkane molecules were truncated at a distance of 12 Å, and were shifted so that the value of the potential at the cutoff distance was zero. Long range corrections to energy or pressure were not applied as our system is a cluster. The interaction potential with the graphite lattice was not truncated.

Earlier simulations[8–10] have used an united atom model to study the melting of butane and hexane monolayers on graphite, and also to study the structure of fluid films of butane and decane as a function of coverage.[19] Such united atom models have also been used to study ultrathin liquid films of *n*-hexadecane on graphite.[24] Here, we have employed an all-atom approach in order to more accurately represent the steric effects that would arise in the solid state. In particular, we have included the explicit interactions of the hydrogen atoms with the graphite which is expected to be a key in the adsorption behaviour of alkanes. Physisorbed layers are a delicate balance of adsorbate and substrate forces and several possible molecular structures and orientations can have comparable energies. Such atomistic details are expected to be significant if we are to reliably calculate the rather subtle structural changes that occur e.g. as a function of coverage. The use of an all-atom model for the study of dense phases of alkanes has been advocated earlier.[25,26]

The initial configurations of the molecules were obtained from the experimental neutron scattering data.[14] In the initial configuration of the three-layer system, the second and third layers were reproductions of the first layer displaced by about 5 Å from the preceding layer. Typically, the systems were equilibrated for around 400 ps at 70 K, and were later subjected to thermal cycling, during which they were annealed at a temperature of 195 K for over 300 ps and were recooled back to 70 K. We believe that this annealing procedure allowed the system to evolve to its thermodynamically stable state without bias from the initial configuration. Structural properties were averaged over a time period of

200 ps at the final temperature of 70 K. In addition, we have adopted a rigorous methodology of performing the simulations for the monolayer and for the multilayer, starting from 'reversed' initial configurations, i.e., simulations were also performed with the monolayer and the multilayer set up initially with intermolecular distances of 4·92 and 5·25 Å respectively. In these simulations with reversed initial configurations, we noticed the sample to get considerably disordered due to annealing at 195 K, and particularly so for the multilayer runs starting from an expanded lattice configuration. In this case, we found that annealing at a slightly reduced temperature of 160 K for about 100 ps retains the ordering of the molecules, as well as enables them to explore the configuration space effectively. The corresponding monolayer configuration was annealed at 195 K for 150 ps. The systems were then slow cooled to 70 K at which temperature they were equilibrated for over 300 ps, followed by runs for structural analyses of duration 200 ps. These runs with 'reversed' initial configurations were performed to test the robustness of the potential of interaction, and the simulation procedures adopted here.

In the following, we present and discuss the results obtained from the MD runs that started from the initial configurations appropriate to the coverage, unless stated otherwise. The structures of the monolayer and the multilayer systems were studied using configurations averaged over time. Instantaneous MD configurations at an interval of 5 ps were stored for analyses, and these were averaged over 150 to 250 ps to obtain the time averaged configurations. Such an averaging procedure is valid and is necessary to analyse the structure of heated crystals. In such situations, analyses of individual snapshots might be misleading due to phase mismatch between the atoms or molecules that need not be exactly at their equilibrium locations due to vibrations. The time-averaging procedure is clearly invalid for molecules that are mobile; in the present case, for molecules in the periphery of the solid cluster. However, in all our analyses, we include *only* those molecules that are present in the core region of the cluster.

We have also calculated the neutron scattering intensity for scattering from the first adsorbed layer for the two coverages. In experiments, the scattering would arise from ordered domains of *n*-hexane which are oriented in different directions. This would amount to powder diffraction from the sample. In the absence of a periodic box, molecules in our simulation get disordered at the periphery of the large cluster. Thus correlations from such molecules should not be included in the calculation of structure factor. In practice, we visually define a large region that is ordered and molecules present within this region are taken to contribute to the structure factor. This rectangular region of linear dimensions around 50 Å, is described by the box lengths, L_x and L_z, with the surface normal along the y direction. Note that this box has to be chosen such that the atomic configuration is periodic with respect to it. The crystal structure factor $F_{hk}(q)$, for a given set of Miller index (h, k) is given by the lattice sum,

$$|F_{hk}|^2 = \left\{\sum_i b_i \cos[2\pi(hs_{x,i} + ks_{z,i})]\right\}^2 + \left\{\sum_i b_i \sin[2\pi(hs_{x,i} + ks_{z,i})]\right\}^2, \tag{1}$$

where $s_{x,j}$ and $s_{z,i}$ are the scaled x and z coordinates of atom i. The scaled coordinates are obtained from dividing the real coordinates by the box lengths defined above. The

neutron scattering lengths are denoted by b_i. In order to make a comparison to experiments in which the samples are deuterated, the scattering lengths are taken to be 6·6484 fm and 6·674 fm for carbon and deuterium atoms respectively. The magnitude of the scattering vector q is given by the expression,

$$q = 2\pi\left[\frac{h^2}{L_x^2} + \frac{k^2}{L_z^2}\right]^{1/2}, \tag{2}$$

and the scattering angle 2θ is obtained from the relation,

$$q = (4\pi \sin\theta)/\lambda, \tag{3}$$

where λ is the wavelength of the neutrons used, which is 2·42 Å. The neutron scattering intensity calculated from MD simulations is a stick pattern in the intensity versus 2θ plot. Convolution of this stick pattern with the instrumental resolution function (lineshape function) leads to a continuous, line broadened intensity profile which can be compared with the experimental profile. The neutron scattering intensities were calculated from the structure factor $F_{hk}(q)$, using such a lineshape function as outlined in Warren[27] and in Kjems *et al*,[28] with the same parameters as that in ref. (28).

In the lattice sum method of calculating the structure factor discussed above, one has to select the periodic box with care. However, the structure factor could as well be calculated from interatomic distances. We have employed the Debye scattering formula[29] to obtain the intensity as,

$$I(q) = \sum_i \sum_j b_i b_j \frac{\sin(qr_{ij})}{qr_{ij}}, \tag{4}$$

where i and j denote atom indices, r_{ij} the distance between them, and the expression is a sum over all such interatomic distances in the system. This expression can be used to obtain the structure factor of a system with no obvious periodicity, or of a crystalline configuration with some amount of disorder. It is also not necessary to define the wave vectors in terms of a periodic box; hence a configuration that includes all the ordered region of the first adsorbed layer can be studied using this relation. We have also calculated the neutron intensities using this procedure including a lineshape analysis as in ref. (28).

3. Results and discussion

The unit cell of *n*-hexane on graphite is experimentally found to be rectangular with lattice parameters 5·30 and 17·04 Å at sub-monolayer coverages and 4·92 and 16·9 Å at multilayer coverages.[10,14] Comparing these unit cell parameters with those of the graphite substrate, we find that at both high and low coverage cases, the a-parameter of the unit cell is a multiple of the underlying graphite substrate, $a_g(\sqrt{3}a_g = 4{\cdot}26$ Å$)$. Only at multilayer coverages is the b-parameter of the unit cell commensurate with the underlying lattice. It is thus evident that there is a uniaxial compression of the lattice

parameter, *b*, which decreases from a value of 5·30 Å for submonolayer coverages to 4·92 Å for multilayer coverages.

It is of interest to follow the evolution of this 'intermolecular' *b*-parameter with coverage. Since we have direct access to real space data in simulations, this change in intermolecular spacing can be easily identified and interpreted in real space. The top view of time averaged configurations of hexane molecules on graphite are shown in figures 1 and 2. In figure 1, we show the configuration of the monolayer at 70 K. Molecules in black have at least one intermolecular distance that is less than 5·0 Å, while the ones depicted in grey have intermolecular distances larger than this cut-off value. The average intermolecular distance in the monolayer along the *x*-axis is found to be 5·31 Å. In figure 2, we show the equivalent data for the three-layered system, where the top view of the first adsorbed layer is shown. The distance cut-off to distinguish between molecules depicted in black and grey is the same as in figure 1. The difference between the two figures is evident; far fewer molecules in the monolayer have an intermolecular distance that is less than 5·0 Å, unlike the case in the multilayer. The average intermolecular distance in the multilayer is found to be 4·93 Å, a value that signifies commensurate adsorption and which is in close agreement with the experimental data.[13,14] From figures 1 and 2, one can also see few molecules that do not belong to the cluster, but yet are physisorbed on the surface, which can be called 'monomeric'. At 70 K, we have found the core region of the first adsorbed layer to be essentially intact, without much loss of molecules to such a monomeric state. This shows that the system appears to be in a

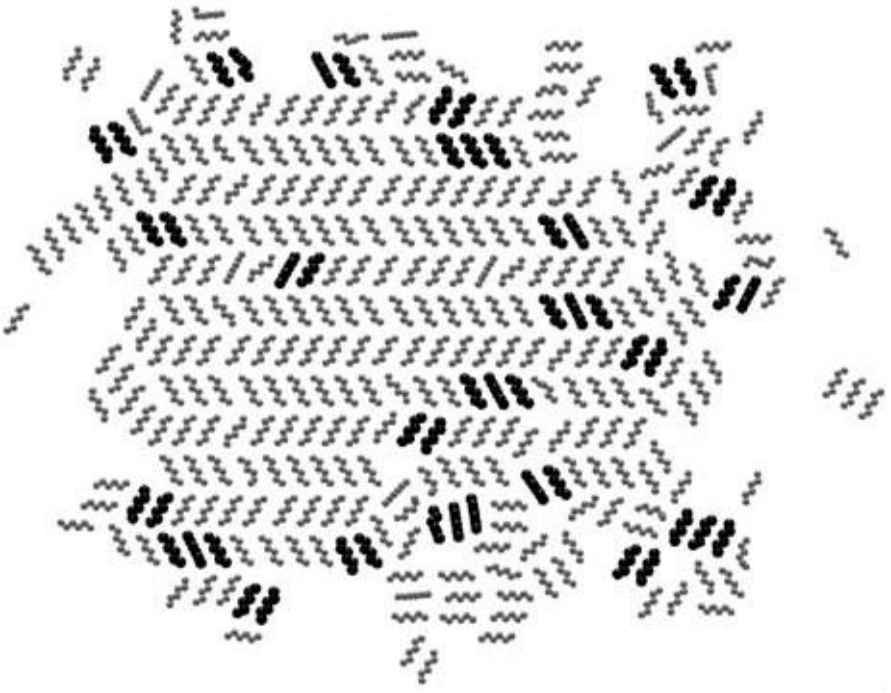

Figure 1. Top view of the time averaged configuration of the *n*-hexane monolayer on graphite. Molecules in black have at least one intermolecular distance that is less than 5·0 Å. Hydrogen atoms are not shown for clarity.

Figure 2. Top view of the time averaged configuration of the first adsorbed layer of *n*-hexane *multilayer* on graphite. Molecules in black have at least one intermolecular distance that is less than 5·0 Å. Hydrogen atoms are not shown for clarity.

steady state within the time scales of the simulation. Additionally, we found no evidence of molecules desorbing from the substrate, even at 195 K.

The reduced intermolecular distance for the multilayer coverage results in an increase in the density of the first adsorbed layer. The number of carbon atoms increases from a value of $0{\cdot}132\,\text{Å}^{-2}$ for monolayer coverage to $0{\cdot}144\,\text{Å}^{-2}$ for the multilayer coverage system, a significant increase of 9%. The compression of the lattice was observed even in a run where the initial configurations were chosen in the reverse manner, i.e., when the monolayer was set up with an initial intermolecular distance of 4·92 Å, and the multilayer was set up with an initial intermolecular distance of 5·25 Å. Averaged configurations for these two cases are shown in figure 3, with the same colouring scheme as used in figures 1 and 2. The monolayer configuration shown in figure 3a, is largely devoid of molecules with intermolecular distances less than 5·0 Å. The average intermolecular distance was found to be 5·21 Å. This monolayer configuration has indeed expanded from its initial lattice constant of 4·92 Å to the value reported above. The multilayer configuration shows the presence of one large region and few small regions containing molecules with intermolecular distances less than 5·0 Å (molecules coloured black). Such regions are interspersed with small pockets of molecules with intermolecular distances larger than 5·0 Å, but much less than the 5·25 Å distance of the monolayer assembly. The average intermolecular distance in the region with black molecules is found to be 4·98 Å. This is a significant reduction when compared to the distance in the initial configuration that was 5·25 Å. It is thus evident that the systems simulated here are robust enough to reproduce the lattice compression despite a drastic change in the initial conditions.

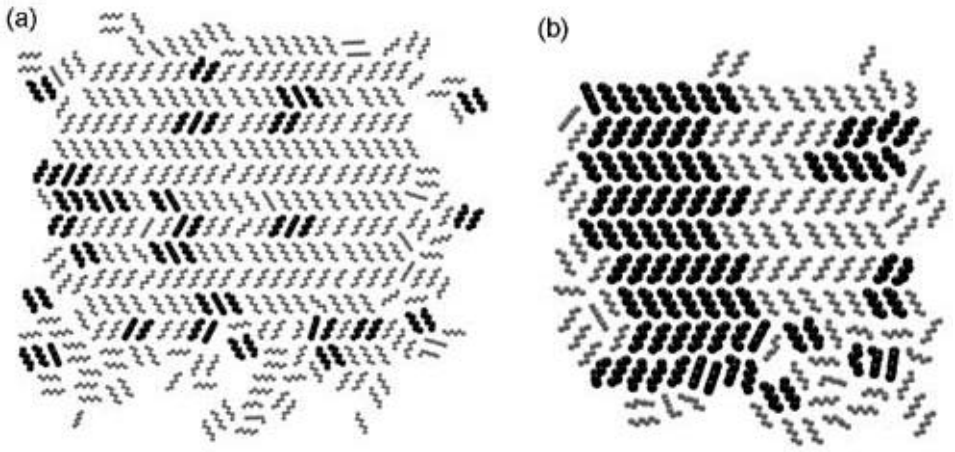

Figure 3. Top view of the time-averaged configuration of the first adsorbed layer of *n*-hexane (**a**) monolayer and (**b**) multilayer on graphite. Here the initial configurations of the two runs were 'reversed', i.e., the monolayer run was started with a compressed lattice, and the multilayer run was started with an expanded lattice. Molecules in black have at least one intermolecular distance that is less than 5·0 Å. Hydrogen atoms are not shown for clarity. The left hand side of the multilayer configuration contains molecules that have commensurately adsorbed to the graphite lattice as a large region.

Thus, our simulations are able to reproduce the two key experimental observations as below.

(i) The compression of the lattice while going from monolayer to multilayer coverages;
(ii) the commensurate adsorption of *n*-hexane for multilayer coverages.

Groszek's model of adsorption of alkanes on graphite predicts the alkane molecules to be oriented with an angle of 30° with respect to the long axis of the alkane unit cell. We have calculated the distribution of this angle (not shown here) for the two systems studied here, and find it to be peaked at an angle of 27°, in close agreement with Groszek's model, and with diffraction experiments that obtain a value of 25°.[13,14]

We next proceed to calculate the neutron scattering intensities. These were obtained from the structure factor using (1) and are shown in figure 4 for both the coverages. The diffraction patterns obtained from simulations are in excellent agreement with experimental values for the peak positions and reasonable agreement for relative intensity. As expected, the peaks in the vicinity of 30° are shifted to higher angles for the multilayer coverage relative to the peak positions for the monolayer due to the compression of the lattice in the *b*-direction. The peak positions and intensities for the two coverages are compared to experiments in tables 1 and 2, where the Miller indices (h, k) for the reflections obtained from simulations are also provided. Note that reflections $(h, 0)$ with h odd, and $(0, k)$ with k odd, are absent, consistent with the experimental identification of *pgg* as the space group. The neutron intensities obtained using a similar procedure for the runs with 'reversed' initial configurations are shown in figure 5. The similarity of the results between the two initial configurations, both for the multilayer and for the monolayer is striking. In calculating the structure factor for the

multilayer with the 'reversed' initial configuration, we included only the large region found on the left hand side of figure 3b that has molecules coloured black. These simulations have indeed been able to reproduce the lattice compression for the multilayer.

For completeness, we compare the results obtained from simulations without periodic boundary conditions with the ones that used them, in figure 6. For the latter, the same procedure as in (1) was used, with the difference that the wave vectors were defined using the simulation box, and not with respect to a periodic lattice defined visually as for the former. The intensities shown in the figure are normalised with respect to the peak at around 33° for the case of multilayers, and with respect to the peak at around 31° for the monolayers. The agreement between the two sets of data is quite good, both for the

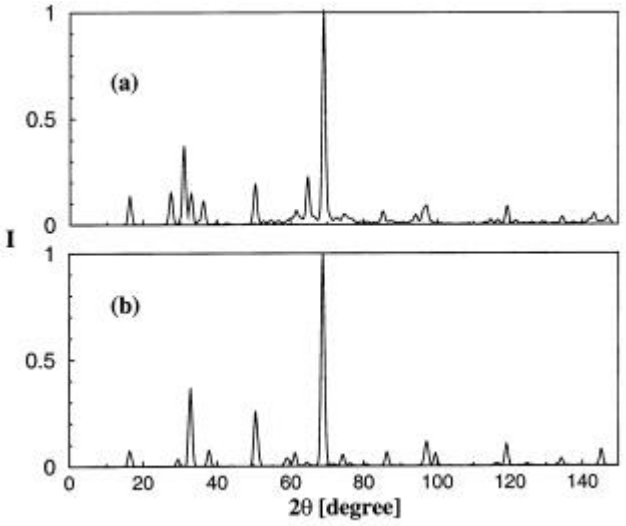

Figure 4. Neutron diffraction intensity as a function of scattering angle obtained from simulations using (1) at the two coverages: (**a**) is for the monolayer and (**b**) is for the multilayer coverage.

Table 1. Peak positions and intensity ratios of calculated neutron scattering data for the *n*-hexane monolayer compared with experiment.[14]

Intensities are normalised with respect to the feature near 31°.

Experiment		Simulation		
$2q$	Intensity	$2q$	Intensity	(h, k)
16·30	0·26	16·30	0·35	(0, 2)
27·77	0·50	27·50	0·40	(1, 1)
31·37	1·00	31·04	1·00	(1, 2)
33·03	0·16	32·95	0·39	(0, 4)
36·40	0·18	36·24	0·29	(1, 3)
50·59		50·35	0·51	(0, 6)
65·31	1·33	64·70	0·59	(2, 4)

Table 2. Peak positions and intensity ratios of calculated neutron scattering data for the first adsorbed layer of a *n*-hexane multilayer system compared with experiment.[14]

Intensities are normalised with respect to the feature near 33°.

Experiment		Simulation		
$2q$	Intensity	$2q$	Intensity	(h, k)
16·37	0·23	16·32	0·20	(0, 2)
29·60	0·40	29·49	0·09	(1, 1)
32·98	1·00	32·98	1·00	(0, 4)
37·82	0·33	37·82	0·21	(1, 3)
50·75	0·63	50·40	0·69	(0, 6)
62·65	0·75	61·19	0·06	(2, 2)

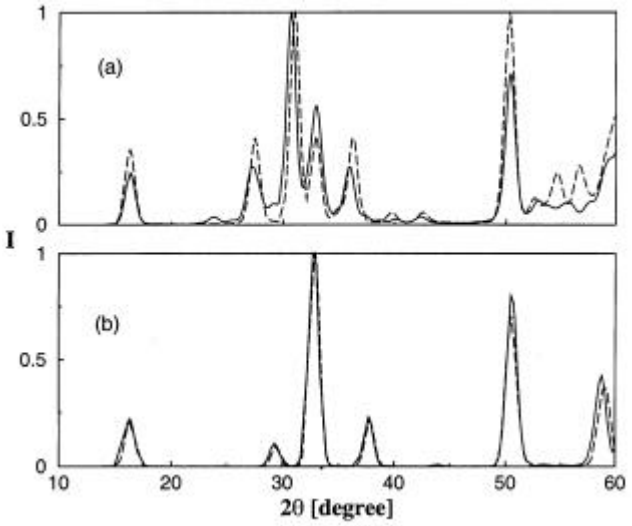

Figure 5. Neutron diffraction intensity as a function of scattering angle obtained from simulations using (1) for the (**a**) monolayer, and (**b**) multilayer systems starting from 'reversed' initial configurations as shown in figure 3. In each of the graphs, the continuous lines are for the 'reversed' initial configurations, and the dashed lines are for normal initial configurations (the latter is the same as in figure 4).

monolayer as well as for the multilayer, signifying that the absence of periodic boundary conditions in our simulations does in no way affect the results.

The neutron intensities obtained using the Debye formula, (4) is shown in figure 7 for the two coverages. The shift in the peak positions as a function of coverage is reproduced, and is in line with the observations in figure 4. The procedures adopted here, both in figure 4 and in figure 7, are able to reproduce the features observed in experiments, although the relative neutron intensities are not in good agreement with

experiments, particularly for the Debye formula where the continuous intensity distribution of the finite sized simulation is not expected to reflect the discrete nature of the intensity distribution of a true lattice with 'Bragg' reflections.

At the low temperature of 70 K, a negligible population of gauche defects in the alkyl chains is to be expected. Our results indicate that indeed, in the ordered regions of the

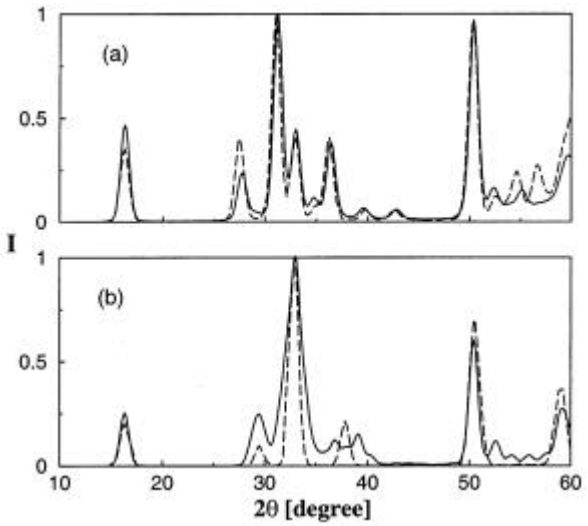

Figure 6. Neutron diffraction intensity as a function of scattering angle obtained from simulations using (1) for the (**a**) monolayer, and (**b**) multilayer systems for the runs with periodic boundary conditions. In each of the graphs, the continuous lines are for the runs with periodic cells, and the dashed lines are for runs with no assumed periodic boundary conditions (the latter is the same as in figure 4).

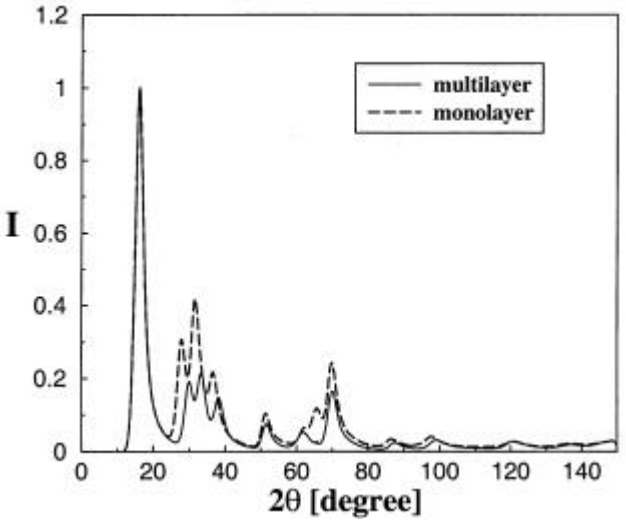

Figure 7. Neutron diffraction intensity as a function of scattering angle using the Debye scattering formula, (4), for the two coverages.

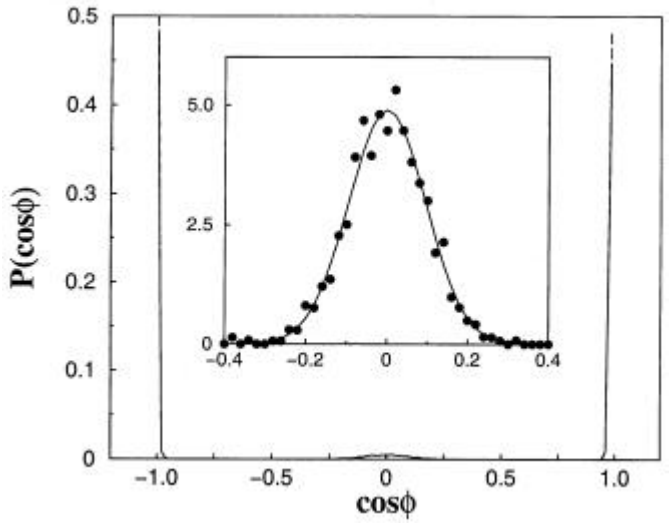

Figure 8. The distribution of the angle, *f*, between the normal of the zig-zag backbone planes of the hexane molecules with the substrate normal. The solid line is for the monolayer and the dashed line is for the first adsorbed layer of the multilayer. The two curves are nearly identical except at cos *f* values around zero. Solid circles in the inset shows the data for cos *f* values around zero in expanded scale (factor of one thousand) for the monolayer, while the corresponding function for multilayers is identically zero. The solid line in the inset is a Gaussian fit to the data and is shown as a guide to the eye.

first adsorbed layer, all molecules are in the *all-trans* conformation. Although gauche defects are not particularly likely, molecular rotations about the long axis are possible. It has been well established by several workers that the preferred configuration of alkane molecules is to have their backbone zig-zag plane parallel to the surface.[10,30,31] We have studied this molecular orientation with respect to the surface. In figure 8, we plot the distribution of the angle made by the normal of the backbone zig-zag planes of the molecules with the surface normal. At the monolayer coverage, one can observe that a few molecules have their backbone plane rotated by 90°, while such excitations are not found in the first adsorbed layer for multilayer coverage. Integration of the data for the monolayer coverage between cos***q*** values of –0·4 to +0·4, shows that around 6% of the molecules are oriented with their backbone planes perpendicular to the surface. This molecular rotation along the long axis possibly decreases the efficiency of packing resulting in an expanded lattice for the monolayer coverage. These molecular rotations are also discernible from the configurations shown in figure 1, where most, but not all, molecules are found to be with their backbone planes parallel to the surface. This is unlike the case of the multilayer coverage (figure 2), where all the molecules in the core region of the cluster are with their backbone planes parallel to the surface. We interpret these changes in molecular orientation to result in the increased compression in the lattice on increasing the coverage. Molecules with backbone planes perpendicular to the surface do not have all their carbon atoms in favourable adsorption sites on the graphite lattice, and are thus not in the ground state.

4. Conclusions

We have been able to observe the structural transition of *n*-hexane adsorbed on the basal plane of graphite, using all-atom molecular dynamics simulations that do not assume any particular periodic cell. We have made two key observations; (i) the uniaxial compression of the lattice, and (ii) the commensurancy of the first adsorbed layer, upon increase in coverage. We have also been able to calculate the neutron diffraction intensities for direct comparison with experiment. Excellent agreement in peak positions, and reasonable agreement in the intensity ratios, with experiments have been obtained. An examination of the angle that the molecular backbone makes with the surface reveals that at monolayer coverage, some molecules tend to rotate such that their zig-zag axis is perpendicular to the surface, while at multilayer coverages, all molecules have their backbone plane parallel to the surface. The latter results in the lattice compression.

Motivated by the results of this study, we plan to extend our calculations to a variety of other adsorbed alkanes. In particular, to those alkanes with an odd number of carbon atoms which have been reported to show additional phase changes in the sub-monolayer region, longer alkanes ($>C_{12}$) which have been reported to have a different plane group to the shorter even alkanes, and binary alkane mixtures.[32]

Acknowledgments

The research reported here was supported in part by grants from the Council of Scientific and Industrial Research, India, and the Leverhulme Trust (SMC), UK. One of the authors (SB) fondly recalls his long association with Professor C N R Rao, and expresses gratitude for his continued encouragement and support.

References

1. Small D M 1986 *The physical chemistry of lipids: From alkanes to phospholipids* (New York: Plenum)
2. Kitaigorodskii A I 1973 *Molecular crystals and molecules* (New York: Academic Press)
3. Groszek A J 1970 *Proc. R. Soc. London* **A314** 473
4. Bhushan B, Israelachvili J N and Landman U 1995 *Nature* (*London*) **374** 607; Gao J, Luedtke W D and Landman U 1997 *J. Chem. Phys.* **106** 4309
5. Rabe J P and Buchholz S 1991 *Science* **253** 424
6. Volkmann U G, Pino M, Altamirano L A, Taub H and Hansen F Y 2002 *J. Chem. Phys.* **116** 2107
7. Castro M A, Clarke S M, Inaba A and Thomas R K 1997 *J. Phys. Chem.* **B101** 8878; Castro M A, Clarke S M, Inaba A, Arnold T and Thomas R K 1998 *J. Phys. Chem.* **B102** 10528; Castro M A, Clarke S M, Inaba A, Arnold T and Thomas R K 1999 *Phys. Chem. Chem. Phys.* **1** 5203
8. Hansen F Y and Taub H 1992 *Phys. Rev. Lett.* **69** 652
9. Herwig K W, Wu Z, Dai P, Taub H and Hansen F Y 1997 *J. Chem. Phys.* **107** 5186
10. Hansen F Y, Newton J C and Taub H 1993 *J. Chem. Phys.* **98** 4128
11. Peters G H and Tildesley D J 1996 *Langmuir* **12** 1557
12. Peters G H 1996 *Surf. Sci.* **347** 169
13. Krim J, Suzanne J, Shechter H, Wang R and Taub H 1985 *Surf. Sci.* **162** 446
14. Arnold T, Thomas R K, Castro M A, Clarke S M, Messe L and Inaba A 2002 *Phys. Chem. Chem. Phys.* **4** 345
15. Krishnan M, Balasubramanian S and Clarke S M 2003 *J. Chem. Phys.* **118** 5082
16. Parrinello M and Rahman A 1980 *Phys. Rev. Lett.* **45** 1196
17. Cheng A and Klein M L 1992 *Langmuir* **8** 2798

18. Clarke S M, Inaba A, Thomas R K and Fish J 2001 *J. Phys. Soc. Jpn*. **A70** 297
19. Leggetter S and Tildesley D J 1989 *Mol. Phys*. **68** 519
20. Martyna G J, Klein M L and Tuckerman M 1992 *J. Chem. Phys*. **97** 2635
21. Tobias D J, Tu K and Klein M L 1997 *J. Chim. Phys. PCB* **94** 1482
22. Steele W A 1973 *Surf. Sci.* **36** 317
23. Vidali G and Cole M W 1984 *Phys. Rev*. **B29** 6736
24. Mundy C J, Balasubramanian S, Bagchi K, Siepmann J I and Klein M L 1996 *Farad. Discuss.* **104** 17
25. Ryckaert J P, McDonald I R and Klein M L 1989 *Mol. Phys*. **67** 957
26. Polson J M and Frenkel D 1999 *J. Chem. Phys*. **111** 1501
27. Warren B E 1941 *Phys. Rev.* **59** 693
28. Kjems J K, Passell L, Taub H, Dash J G and Novaco A D 1976 *Phys. Rev*. **B13** 1446
29. Elliott S R 1998 *The physics and chemistry of solids* (New York: Wiley) p. 114
30. Herwig K W, Newton J C and Taub H 1994 *Phys. Rev*. **B50** 15287
31. Balasubramanian S, Klein M L and Siepmann J I 1995 *J. Chem. Phys*. **103** 3184
32. Inaba A, Clarke S M, Arnold T and Thomas R K 2002 *Chem. Phys. Lett*. **352** 57